DALTON
FULL PAPER

Thermodynamic and fluorescence emission studies on chemosensors containing anthracene fluorophores. Crystal structure of $\{[CuL^1Cl]Cl\}_2 \cdot 2H_2O$ [L^1 = *N*-(3-aminopropyl)-*N*′-3-(anthracen-9-ylmethyl)aminopropylethane-1,2-diamine]

Mª Alexandra Bernardo,[a] Fernando Pina,*[a] Beatriu Escuder,[b] Enrique García-España,*[c] Mª Luz Godino-Salido,[d] Julio Latorre,[c] Santiago V. Luis,*[b] José A. Ramírez[c] and Conxa Soriano[e]

[a] *Departamento de Química, Centro de Química Fina e Biotecnologia, Faculdade de Ciencias e Tecnologia, Universidade Nova de Lisboa, Monte de Caparica, Portugal*
[b] *Departamento de Química Inorgánica y Orgánica, Laboratorio de Química Orgánica, Universitat Jaume I, 12080 Castellón, Spain*
[c] *Departament de Química Inorgánica, Facultat de Química, Universitat de València, C/ Dr. Moliner 50, 46100 Burjassot (Valencia), Spain. E-mail: enrique.garcia-es@uv.es*
[d] *Departamento de Química Inorgánica y Orgánica, Universidad de Jaén, 23071 Jaén, Spain*
[e] *Departament de Química Orgánica, Facultat de Farmacia, Universitat de València, Av. Vicente Andrés Estellés s/n, 46100 Burjassot (València), Spain*

Received 5th November 1998, Accepted 20th January 1999

The co-ordination capabilities toward hydrogen ions, Co^{2+}, Ni^{2+}, Cu^{2+}, Zn^{2+} and Cd^{2+} of the novel receptor 2,6,9,13-tetraaza[14](9,10)anthracenophane (L) and of its open-chain counterpart *N*-(3-aminopropyl)-*N*′-3-(anthracen-9-ylmethyl)aminopropylethane-1,2-diamine (L^1) is described. Stepwise protonation constants of the cyclic receptor (L) are lower than those of the open-chain receptor (L^1) . Quenching effects of the fluorescence emission occur upon first and second deprotonation of L and upon second deprotonation of L^1. Stability constants of the Co^{2+}, Ni^{2+}, Cu^{2+}, Zn^{2+} and Cd^{2+} complexes follow the Irving–Williams trend and are intermediate between those of triethylenetetra-amine with terminal primary amino groups and those of the α,ω-dibenzylated receptor 1,12-dibenzyl-1,5,8,12-tetraazaciclododecane. Luminescence studies show that complexation of Cu^{2+} and Ni^{2+} by L^1 yield CHEQ effects (chelation enhanced quenching) while complexation of Zn^{2+} and Cd^{2+} produce CHEF effects (chelation enhanced fluorescence). The magnitude of these effects depends on the strength of the co-ordination. Crystals of $\{[CuL^1Cl]Cl\}_2 \cdot 2H_2O$ are triclinic, space group $P\bar{1}$, with $a = 13.307(1)$, $b = 13.305(1)$, $c = 16.538(2)$ Å, $\alpha = 104.94(1)$, $\beta = 111.67(1)$, $\gamma = 102.76(1)^\circ$, $R_1 = 0.0885$, $wR_2 = 0.2667$. The crystal structure of $\{[CuL^1Cl]Cl\}_2 \cdot 2H_2O$ shows a very strongly axially distorted square pyramidal co-ordination geometry in which the Cu^{2+} cation is co-ordinated by all the nitrogen donors of the receptor and a chloride ion disposed at the apical position of the square pyramid. The asymmetric unit is formed by two slightly different $[CuL^1Cl]^+$ cations with an arrangement that shows π-stacking of their anthracene sub-units.

Introduction

The construction of molecular devices aiming at detecting and/or removing traces of metal ions is a topic of general interest in chemistry. Today this goal has reached special relevance owing to the greater awareness about environmental hazards caused by heavy and/or toxic metals.

Supramolecular and co-ordination chemistry can offer interesting approaches in this respect.[1–3] Supramolecular detection devices can be made by assembling control units for the interaction with given substrates and signalling units for communicating that the interaction has occurred. The signalling unit should possess properties whose magnitudes are deeply affected following the substrate–receptor event. In this context, one of the properties most widely used has been fluorescence emission, since it provides fast and easily measurable responses to chemical stimuli. Several research groups have broadly explored this field over recent years.[4–10]

Recently we have reported on a series of new chemosensors containing a polyamine fragment as control unit and one or two benzene units as fluorophores (see, for example, receptors L^3 and L^4). The effects of the proton transfer and metal complex formation reaction on the fluorescent behaviour of these compounds were studied.[11,12]

Here, we report on the new related macrocyclic receptor L in which the aromatic benzene ring has been replaced by anthracene in order to improve the efficiency of the device. Also, to allow comparison we have re-prepared its open-chain counterpart (L^1)[6] and present a thermodynamic and fluorescence emission study on their proton and metal ion binding characteristics. CHEF (chelation enhanced fluorescence) or CHEQ (chelation enhanced quenching) effects are observed depending on the co-ordinated substrate. Also we show that luminescence measurements can complement the potentiometric technique in order to determine, or estimate association constants, mainly, when the application of potentiometry is hindered due, for instance, to solubility limits. Additionally, we present the results of the X-ray diffraction characterisation of the Cu^{2+} complex $\{[Cu(L^1)Cl]Cl\}_2 \cdot 2H_2O$.

Experimental

Synthesis of 2,6,9,13-tetraaza[14](9,10)anthracenophane (L) †

Anthracenophane L was obtained by one-pot cyclisation and

---

† The name for this compound follows the abbreviated nomenclature proposed for cyclophanes in: F. Diederich, *Cyclophanes*, The Royal Society of Chemistry, Cambridge, 1991.

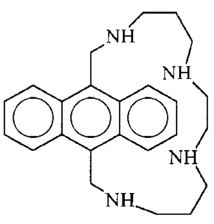

L

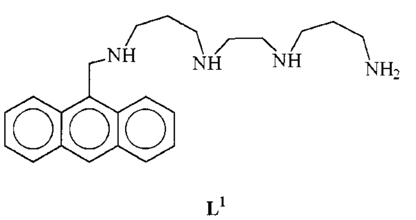

L^1

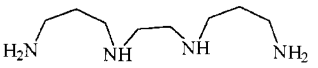

L^2

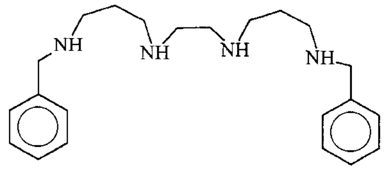

L^3

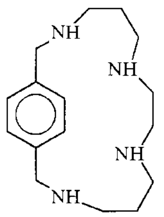

L^4

deprotection from *N*,*N*′,*N*″,*N*‴-tetrakis(*o*-nitrobenzenesulfonyl)-1,5,8,12-tetraazadodecane and 9,10-bis(bromomethyl)-anthracene.[13] Thus, the *o*-nosylated polyamine and the dibromide were heated in DMF at 100 °C for three days using an excess of K_2CO_3 as a base. The resulting mixture was cooled and deprotection was carried out by addition of 10 equivalents of $HSCH_2CH_2OH$ and stirring for 15 h at room temperature. After isolation and chromatographic purification [MeOH–NH_3 (aq), 10 : 0.5] compound L was obtained as a waxy solid in 30% yield and was characterised as its tetrahydrochloride salt. NMR (D_2O): ^{1}H, δ 1.63 (m, 4H), 2.53 (t, 4H), 2.7 (t + s, 8H), 4.9 (s, 4H), 7.7 (m, 4H), 8.1 (m, 4H); ^{13}C, δ 22.9, 42.5, 43.5, 44.3, 45.0, 124.9, 128.8, 131.0 (Found: C, 54.8; H, 6.8; N, 10.9. Calc. for $C_{24}H_{36}N_4Cl_4$: C, 55.2; H, 6.9; N, 10.7%).

N-(3-aminopropyl)-*N*′-3-(anthracen-9-ylmethyl)aminopropylethane-1,2-diamine (L^1)

This compound was prepared by a modification of the procedure reported in ref. 6. 1,5,8,12-Tetraazadodecane (1.78 g, 10 mmol) and anthracene-9-carbaldehyde (0.41 g, 2 mmol) were dissolved in ethanol (40 mL) and allowed to react for 48 h at room temperature. Then, $NaBH_4$ (0.9 g, 20 mmol) was added portionwise and the resulting solution warmed at 50 °C for 4 h. Ethanol was distilled off under reduced pressure, the residue treated with water (20 mL) and extracted with dichloromethane (2 × 15 mL). Then, it was dried over Na_2SO_4 and the solvent removed by rotary evaporation. The residue was dissolved in ethanol and treated with excess aqueous 48% HBr. The yellowish precipitate formed was filtered off and dried under vacuum. Yield 45%, mp 254–256 °C. NMR (D_2O): ^{1}H, δ 1.96–1.99 (m, 4H), 2.94–3.30 (m, 8H), 3.35 (s, 4H), 4.93 (s, 2H), 7.42 (t, 2H), 7.53 (t, 2H), 7.90 (d, 2H), 8.00 (d, 2H), 8.36 (s, 1H); ^{13}C, δ 23.2, 24.3, 37.0, 43.3, 43.6, 45.0, 45.6, 45.7, 120.2, 122.9, 125.8, 128.1, 129.8, 130.3, 130.7, 130.8 (Found: C, 39.8; H, 5.4; N, 8.0. Calc. for $C_{23}H_{36}N_4Br_4$: C, 40.1; H, 5.2; N, 8.1%).

Materials

All the measurements were carried out in 0.15 mol dm^{-3} NaCl. CO_2-free NaOH, HCl, or $HClO_4$ solutions were prepared following the procedure reported in ref. 14.

Spectrophotometric and spectrofluorimetric titrations

Absorption spectra were recorded on a Perkin-Elmer Lambda 6 spectrophotometer and fluorescence emission on a SPEX F111 Fluorolog spectrofluorimeter. $HClO_4$ and NaOH were used to adjust the pH values that were measured on a Metrohom 713 pH meter. All measurements were carried out in 0.15 mol dm^{-3} NaCl. The linearity of the fluorescence emission with concentration was checked in the concentration range used (2×10^{-5}–2×10^{-6} mol dm^{-3}). Spectrophotometric titrations have also been performed. The absorbance of the excitation wavelength was maintained lower than 0.15. When excitation was carried out at wavelengths different than the isobestic points, a correction for the absorbed light was performed.

Potentiometry

The potentiometric titrations were carried out at 298.1 ± 0.1 K. NaCl (0.15 mol dm^{-3}) was used as supporting electrolyte owing to the low solubility of the complexes in $NaClO_4$. The experimental procedure and the potentiometric equipment (burette, potentiometer, cell, stirrer, microcomputer, *etc.*) have been fully described elsewhere.[15] The acquisition of the emf data was performed with the computer program PASAT.[16] The reference electrode was an Ag/AgCl electrode in saturated KCl solution. The glass electrode was calibrated as a hydrogen-ion concentration probe by titration of previously standardised amounts of HCl with CO_2-free NaOH solutions. The equivalent point was determined by Gran's method,[17] which gives the standard potential, $E°'$, and the ionic product of water [$pK_w = 13.73(1)$]. The concentrations of the different metal ions employed were determined gravimetrically by standard methods.

The computer program HYPERQUAD[18] was used to calculate the protonation and stability constants. The titration curves for each system (*ca.* 100 experimental points corresponding to at least three measurements, pH range investigated 2.5–10.5, concentration of metals and L ranging from 1×10^{-3} to 5×10^{-3} mol dm^{-3}) were treated either as a single set or as separated curves without significant variations in the values of the stability constants. Finally, the sets of data were merged together and treated simultaneously to give the final stability constants. For the Ni^{2+} systems, a delay of several minutes before each reading was adopted in order to reach equilibrium. Moreover, several measurements were made both in formation and in dissociation (from acid to alkaline pH and *vice versa*) to check the reversibility of the reactions.

EHMO Calculations

All calculations were performed by using a package of programs for molecular orbital analysis by Mealli and Proserpio,[19] based on CDNT (atomic cartesian co-ordinate calculations), ICON (extended Huckel method with the weighted H_{ij} formula) and FMO (fragment molecular orbital), including the drawing program CACAO (computerised aided composition of atomic orbitals).

X-Ray structure analysis

Crystals of $\{[Cu(L^1)Cl]Cl\}_2\cdot 2H_2O$ suitable for X-ray diffraction analysis were obtained by slow evaporation at pH 8 of aqueous solutions of $CuCl_2\cdot 4H_2O$ (10^{-2} mol dm^{-3}) and L^1 (10^{-2} mol dm^{-3}) in the presence of an excess of NaCl.

Crystal data. $C_{46}H_{64}Cl_4Cu_2N_8O_2$, $M = 1029.93$, triclinic, space group $P\bar{1}$, $a = 13.307(1)$, $b = 13.305(1)$, $c = 16.538(2)$ Å, $\alpha = 104.94(1)$, $\beta = 111.67(1)$, $\gamma = 102.76(1)°$, $Z = 2$, $V = 2460(1)$ Å^3, $T = 298$ K, μ(Mo-Kα) = 1.9 mm^{-1}, 8645 reflections measured, 4844 unique ($R_{int} = 0.0885$) which were used in all calculations. The final $wR(F^2)$ was 0.099.

A violet–blue well formed single crystal of $\{[Cu(L^1)Cl]Cl\}_2\cdot 2H_2O$ (approximate size 0.15 × 0.15 × 0.20 mm) was mounted on an ENRAF-NONIUS CAD-4 X-Ray single crystal diffractometer ($\lambda = 0.71073$ Å). The unit cell dimensions were measured from the angular settings of 25 reflections with θ between 15 and 25°. The reflections were measured in the

Table 1 Stepwise stability constants of receptors L and L^1 determined at 298.0 + 0.1 K in 0.15 mol dm^{-3} NaCl by potentiometry (pot) and fluorescence emission titrations (em). Stability constants for polyamines L^2, L^3 and L^4 taken from refs. 27,12(*a*) and 11 are also included

	L		L^1				
Reaction[a]	Pot[b]	Em[c]	Pot	Em	L^2	L^3	L^4
$H + L = HL$	10.08(2)	10.0	10.28(2)	10.3	10.53	9.68	9.93
$H + HL = H_2L$	8.69(2)	9.5	9.21(1)	9.3	9.77	8.87	9.09
$H + H_2L = H_3L$	6.90(3)	7.0	7.65(2)	7.9	8.30	7.37	7.44
$H + H_3L = H_4L$	3.90(5)	4.0	5.59(3)	5.6	5.59	4.90	3.61
$\log(\Sigma K_{H_jL})$	29.6		32.7		34.2	30.8	30.0

[a] Charges are omitted for clarity. [b] Values in parentheses are standard deviations in the last significant figure. [c] Estimated errors ±0.1.

Table 2 Stability constants for the interaction of receptor L^1 with Co^{2+}, Ni^{2+}, Cu^{2+}, Zn^{2+} and Cd^{2+} determined in 0.15 mol dm^{-3} NaCl at 298.0 ± 0.1 K by potentiometry (pot) and fluorescence emission titrations (em)

	Co^{2+}	Ni^{2+}		Cu^{2+}		Zn^{2+}		Cd^{2+}	
Reaction[a]	Pot	Pot	Em	Pot	Em	Pot	Em	Pot	Em
$M + L = ML$	7.95(1)[b]	11.61(2)	10.0	19.45(1)	19.5	8.62(1)	8.6	8.20(2)	8.2
$ML + H = MHL$	7.75(2)	6.18(1)	>6.5	4.31(1)	>5.0	7.35(1)	7.4	7.61(4)	7.6
$M + HL = MHL$	5.40	7.50		13.47		5.68		5.52	
$ML + OH = ML(OH)$	3.64(1)					3.82(2)	3.7		

[a] Charges are omitted for clarity. [b] Values in parentheses are standard deviations on the last significant figure.

hkl range (−15, −15, 0) to (15, 15, 19) between limits $1 < \theta < 25°$. The ω–2θ scan technique and a variable scan rate with a maximum scan time of 60 s per reflection were used. The intensity of the primary beam was checked throughout the data collection by monitoring three standard reflections every 3600 s. The final drift correction factors were in the range 0.98 and 1.02. Profile analysis was performed on all reflections,[20] a semiempirical absorption correction, ψ-scan based, was performed.[21] In total, there were 8645 reflections, of which 4844 had $F_o > 4\sigma(F_o)$. Lorentz and polarisation corrections were applied and the data were reduced to F_o^2 values. The structure was solved by the Patterson method using the program SHELXS-86[22] running on an IBM Pentium MMX 200 computer. Isotropic least-squares refinement was performed by means of the program SHELXL-93.[23] Hydrogen atoms were placed in calculated positions. During the final stages of the refinement the positional parameters and the anisotropic thermal parameters of the non-hydrogen atoms were refined. The hydrogen atoms were refined with a common thermal parameter. The final conventional agreement factors were $R_1 = 0.0885$ and $wR_2 = 0.2667$. The maximum shift of esd ratio in the last full matrix least-squares cycle was 0.001. The final difference Fourier map showed no peaks higher than 1.43 e $Å^{-3}$ or deeper than −0.65 e $Å^{-3}$. Atomic scattering factors were taken from ref. 24. The molecular plots were produced by the program ORTEP.[25]

CCDC reference number 186/1325.

See http://www.rsc.org/suppdata/dt/1999/915/ for crystallographic files in .cif format.

Results and discussion

Acid–base behaviour

The logarithms of the stepwise protonation constants of anthracenophane L and of its open-chain analogue L^1 are shown in Table 1. For comparison the basicity constants of some related receptors with the same set of hydrocarbon fragments between the nitrogen atoms are also included in Table 1.[12,26,27] It is interesting to note the good agreement between the protonation constants determined by potentiometry and those obtained from the fluorescence measurements following the procedure reported in ref. 12(*a*) (Table 1).

First, it should be noted that the cyclic anthracenophane ligand L displays lower basicity than L^1. This can be attributed to the cyclic topology that yields a reduction in conformational freedom of the receptor and therefore, charged polyammonium groups cannot be as far away from each other as in the open-chain ligand. This is particularly reflected in the value of the constant of the last protonation step, which for the cyclic ligand is two orders of magnitude lower than for L^1. Other aspects that should be considered for interpreting basicity trends are the nature of the nitrogen atoms as well as the hydrophilic–hydrophobic characteristics of the molecule.[28] In this sense, comparison of receptors L and L^1 with polyamines L^2–L^4 containing different nitrogen atoms and/or hydrophobic moieties is of interest. Indeed, a plot of the overall basicities of all these ligands shows that L^1, L^2 and L^3 lie on a straight line with their basicities in the order $L^2 > L^1 > L^3$ (Table 1). So, the higher the number of primary amino groups in the molecule the greater the basicity found, as expected from the hydration characteristics of the different amino groups. Macrocycles L and L^4 display similar basicities with that for L^4 being slightly higher, both being lower than those for the open-chain polyamines. The slightly higher basicity of L^4 with respect to L is probably due to the greater hydrophobicity of the anthracene fragment.

Finally, the sequence of the values of the stepwise constants, two large constants, one intermediate and the final one much lower (particularly for L) can be explained taking into account criteria of minimum electrostatic repulsions between like charges as already discussed for L^3 and L^4.[12,26,27]

Metal co-ordination

Table 2 lists logarithmic stability constants for the interaction of L^1 with transition metal ions Co^{2+}, Ni^{2+}, Cu^{2+} and post-transition ions Zn^{2+} and Cd^{2+} determined in 0.15 mol dm^{-3} NaCl at 298.0 ± 0.1 K.

The low water-solubility of the metal complexes of L prevented determination pH-metrically of their stability constants. However, it has been possible to obtain estimations of these constants by spectrofluorimetric techniques (*vide infra*). For the Ni^{2+}, Cu^{2+}, Zn^{2+} and Cd^{2+} complexes of L^1, there is a reasonable agreement between the potentiometric values of the formation constants and those obtained by the emission fluorescence measurements [Table 2, ref. 12(*c*)].

An analysis of the magnitudes of the stability constants with respect to those of related ligands may provide a connection with respect to the number of nitrogen atoms in the first co-ordination sphere. In Fig. 1 the values of the constants for the

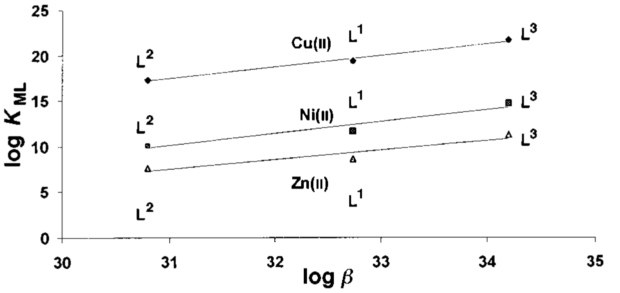

Fig. 1 Plot of the formation constants for the $[ML]^{2+}$ complexes of Cu^{2+}, Ni^{2+} and Zn^{2+} for L^1, L^2 and L^3 as a function of the overall basicity of the receptors ($\log\beta = \sum \log K_{\mathrm{H}_i\mathrm{L}}$).

$[ML]^{2+}$ copper, nickel and zinc complexes of ligands L^1, L^2 and L^3 are plotted *vs.* the cumulative basicities of the receptors. Examination of Fig. 1 shows that the stability of the metal ion complexes of L^1 is intermediate between those of the complexes of triethylenetetraamine and those of the complexes of the terminally N-benzylated receptor L^3.[12b,27] Also the differences in selectivity in the co-ordination to the metal ions should not be very large owing to the linear relationship obtained between the stability of the complexes and overall basicity of the receptors. On the other hand, the stability constants for the $[ML]^{2+}$ and $[M(HL)]^{3+}$ complexes of the different metal ions follow the Irving–Williams trend.

These data seem to indicate that all nitrogen donors are involved in the first co-ordination sphere of the metals as is also suggested by the lack of hydroxylated species at low pH values. Indeed, such hydroxylated species are only found for Co^{2+} and Zn^{2+} complexes and present large pK_a values ($\log K_{\mathrm{ML/ML(OH)}\cdot\mathrm{H}}$, $Co^{2+} = -10.09$, $Zn^{2+} = -9.91$), which suggest low polarisation of the co-ordinated water molecules and indicate the co-ordination of all nitrogen atoms to the metal ions. The higher limit of *ca.* 15 logarithmic units estimated by fluorescence for the constant of the Cu^{2+} complex of receptor L, is dramatically lower than the constants for any of the above open-chain tetraamines. This value is even lower than for complexes of saturated azamacrocycles, such as cyclam or cyclen,[27] that involves all their four nitrogen donors in the co-ordination to copper(II). However, such an estimate of the stability constant is close to the stability values obtained for analogous [1 : 1]cyclophanes such as 2,6,9,13-tetraaza[14]paracyclophane (L^4) or 16,17,19,20-tetramethyl-2,6,9,13-tetraaza[14]paracyclophane, for which it has been extensively proved that only three out of its four nitrogen atoms are involved in the co-ordination to different metal ions such as Cu^{2+} and Zn^{2+} or even Hg^{2+}.[26,29–31] The aromatic spacers in those receptors preclude simultaneous involvement of both benzylic nitrogen atoms in the co-ordination to a single metal ion. Accordingly, just three of the nitrogens in L form part of the first co-ordination of its metal complexes.

Crystal structure of $\{[Cu(L^1)Cl]Cl\}_2\cdot H_2O$ 1

The unit cell of complex **1** consists of four $[CuL^1Cl]^+$ cations, four chloride anions and lattice water molecules. Two $[CuL^1Cl]^{2+}$ cations form the asymmetric unit, which are fairly similar to each other (Fig. 2). Each Cu^{2+} is bonded to all four nitrogen donors of the polyamine in a square planar fashion with a chloride atom in the apical position of a square-pyramid showing a large Jahn–Teller distortion. The Cu–N bond distances range from 2.010(7) for Cu(1)–N(1) to 2.060(6) Å for Cu(1)–N(4) while the Cu–Cl distances are 2.624 Å in both cations (Table 3). The angles in the basal plane vary from 84.4(2) to 92.2(3)° and the elevation of the Cu^{2+} macrocycle above the mean average plane defined by the nitrogens of the receptor is 0.11 Å. The anthracene rings in both cations are almost parallel to each other [5.9(2)°] with staggered orientation; the distances between both anthracene fragments vary from 3.6 to 4.0 Å, which indicate stacking interactions that contribute to organise the crystal packing (Fig. 3).

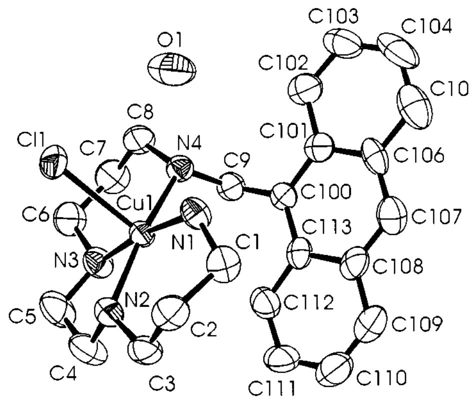

Fig. 2 ORTEP drawing of the $[CuL^1Cl]^{2+}$ cation. Thermal ellipsoids are drawn at the 30% probability level.

Table 3 Selected bond lengths (Å) and bond angles (°) for $\{[CuL^1Cl]Cl\}_2\cdot 2H_2O$

Cu(1)–N(1)	2.010(7)	Cu(2)–N(5)	2.018(6)
Cu(1)–N(2)	2.030(6)	Cu(2)–N(6)	2.033(6)
Cu(1)–N(3)	2.042(7)	Cu(2)–N(7)	2.034(6)
Cu(1)–N(4)	2.060(6)	Cu(2)–N(8)	2.057(6)
Cu(1)–Cl(1)	2.624(2)	Cu(2)–Cl(2)	2.624(2)
N(1)–Cu(1)–N(2)	92.0(3)	N(5)–Cu(2)–N(6)	92.2(3)
N(1)–Cu(1)–N(3)	172.2(3)	N(5)–Cu(2)–N(7)	172.5(3)
N(2)–Cu(1)–N(3)	84.4(3)	N(6)–Cu(2)–N(7)	84.5(3)
N(1)–Cu(1)–N(4)	91.5(3)	N(5)–Cu(2)–N(8)	91.5(2)
N(2)–Cu(1)–N(4)	170.4(3)	N(6)–Cu(2)–N(8)	170.6(3)
N(3)–Cu(1)–N(4)	91.0(3)	N(7)–Cu(2)–N(8)	90.8(3)
N(1)–Cu(1)–Cl(1)	90.0(2)	N(5)–Cu(2)–Cl(2)	89.8(2)
N(2)–Cu(1)–Cl(1)	95.2(2)	N(6)–Cu(2)–Cl(2)	94.9(2)
N(3)–Cu(1)–Cl(1)	97.2(2)	N(7)–Cu(2)–Cl(2)	97.2(2)
N(4)–Cu(1)–Cl(1)	93.7(2)	N(8)–Cu(2)–Cl(2)	93.8(2)

Absorption and fluorescence emission

Effect of protons. The absorption spectra of chemosensors L and L^1 are only slightly affected by the protonation of their polyammonium receptor moieties, and the shape and position of the bands in these spectra are very similar to those in the spectrum of the anthracene chromophore. On this basis, the light absorption process is likely centered in the π–π^* absorption band of the anthracene over the pH range investigated. By contrast the fluorescence emission is drastically affected by the protonation state of the receptor (Fig. 4).

In both sensors, the maximum of the fluorescence emission intensity is observed for the fully protonated form. This behaviour is due to the well documented fact that deprotonated amines are able to quench, by inter- or intra-molecular electron transfer, the excited state of many aromatic compounds including anthracene. According to ^1H NMR data for both compounds, the first proton to be removed upon increasing the pH belongs to the central ethylenediamine fragment of the receptor. For instance, in L^1 the resonances of the central carbon atoms move significantly upfield in the pH range where the third and fourth protonation occur.[28] However, owing to their different molecular topologies, in L the distance of the central nitrogen lone pairs to the anthracene chromophore is smaller and thus the quenching effect is larger than in L^1. Upon removal of the second proton, both compounds show the same protonation state with the lone pairs of the central nitrogens deprotonated. This proton arrangement increases the probability of the intramolecular electron transfer quenching process. These results are in agreement with our previous work with N,N′-dibenzylated tetraamines and tetraazacyclophanes,

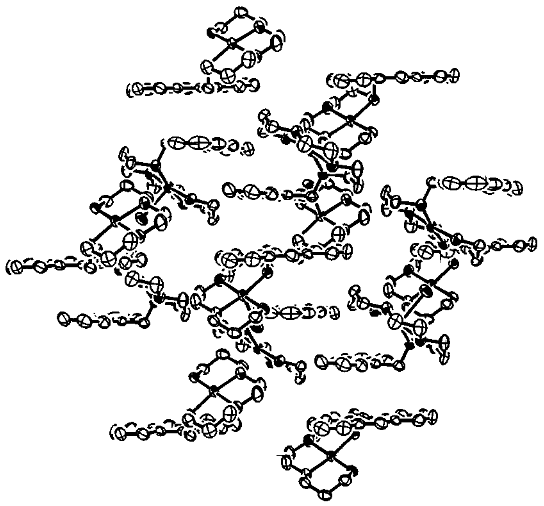

Fig. 3 ORTEP drawing of a portion of the packing for the {[CuL^{1}Cl]-Cl}$_2$ complex. Thermal ellipsoids are drawn at the 30% probability level.

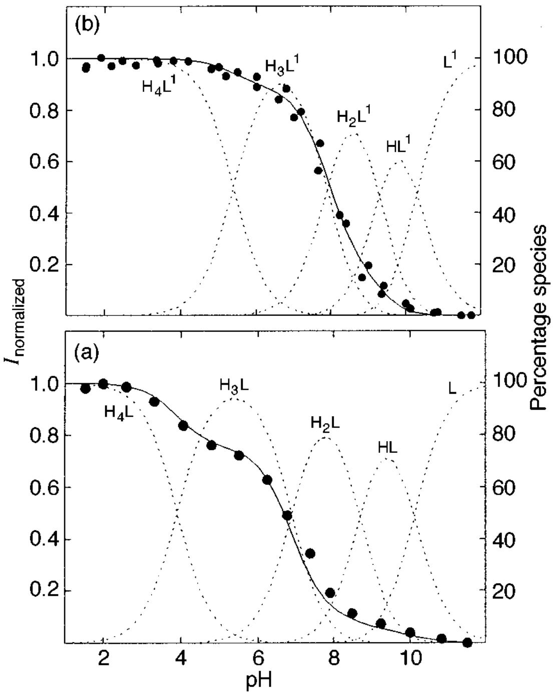

Fig. 4 Steady-state fluorescence emission titration curves (——) of (a) L and (b) L^1. Molar fraction distribution of the protonated species are also represented (·····).

which show the same behaviour.[11,12] At this stage the fluorescence emission is almost completely quenched.

In conclusion, the most significant difference in these two compounds is the fact that in L the central nitrogens are forced by the structure to remain near the chromophore unit favouring the efficiency of the electron transfer process.

Effect of metals. Chemosensor L^1 is sensitive not only to protons but also to the co-ordination of metal ions. Depending on the metal, a chelation-enhanced fluorescence (CHEF) or a chelation-enhanced quenching (CHEQ) occur. Fig. 5 shows examples of these two effects.

CHEQ effects. For Cu^{2+}, the absorption spectra is largely affected by the metal co-ordination, with the appearance of a typical charge transfer absorption band. Molecular orbital calculations show that while in the free fully protonated ligand, both the HOMO and LUMO are located in the anthracene, for [CuL^1]$^{2+}$ a partially occupied orbital exhibiting metal contribution, appears in the middle of the ligand orbitals (Fig. 6).

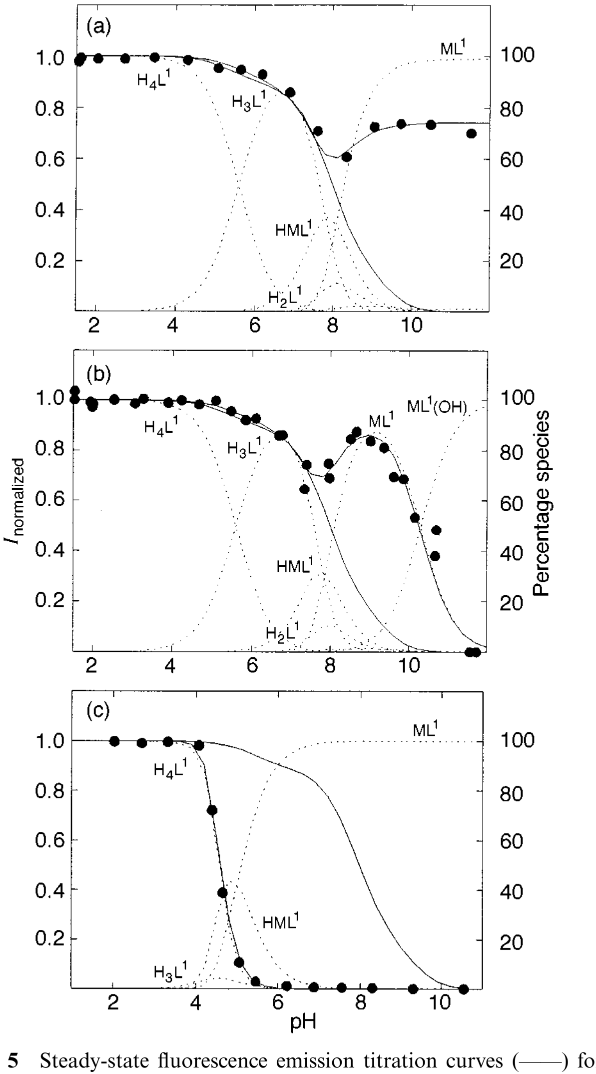

Fig. 5 Steady-state fluorescence emission titration curves (——) for ML^1 complex species: (a) Cu^{2+} complexes, (b) Zn^{2+} complexes, (c) Cd^{2+} complexes. Molar fraction distribution of the protonated species are also represented (·····).

These calculations not only affirm that in the free ligand the absorption band is centered in the anthracene chromophore, but also the appearance of a charge transfer band in the electronic absorption spectrum of the Cu^{2+} complex. By contrast, for the complexes [ZnL^1]$^{2+}$ or [CdL^1]$^{2+}$, the HOMO and LUMO are similar to the free ligand, and no charge transfer is expected.

The fluorescence emission of the sensor L^1 upon complexation with copper is shown in Fig. 5(a). According to the potentiometric data, formation of the species [Cu(HL^1)]$^{3+}$ and [CuL^1]$^{2+}$ was observed. Inspection of Fig. 5(a) indicates that neither of these metal–complex species are emissive. A possible explanation for the quenching effect is energy transfer involving copper, as observed by other authors.[5]

For Ni^{2+}, identical species are formed and the behaviour seems to be similar to that for Cu^{2+} albeit with slightly smaller association constants. Thus the pH dependent molar fraction distribution of the free ligand emissive species as well as the global pattern of the titration curves is only slightly affected.

CHEF effects. For complexes between Zn^{2+} and L^1 the potentiometric data is compatible with the formation of the species [Zn(HL^1)]$^{3+}$, [ZnL^1]$^{2+}$ and [ZnL^1(OH)]$^+$. As shown in Fig. 5(b) only the first two species are emissive. In previous work carried out with N,N′-dibenzylated polyamines and polyazacyclophanes sensors,[11,12] we have already observed that

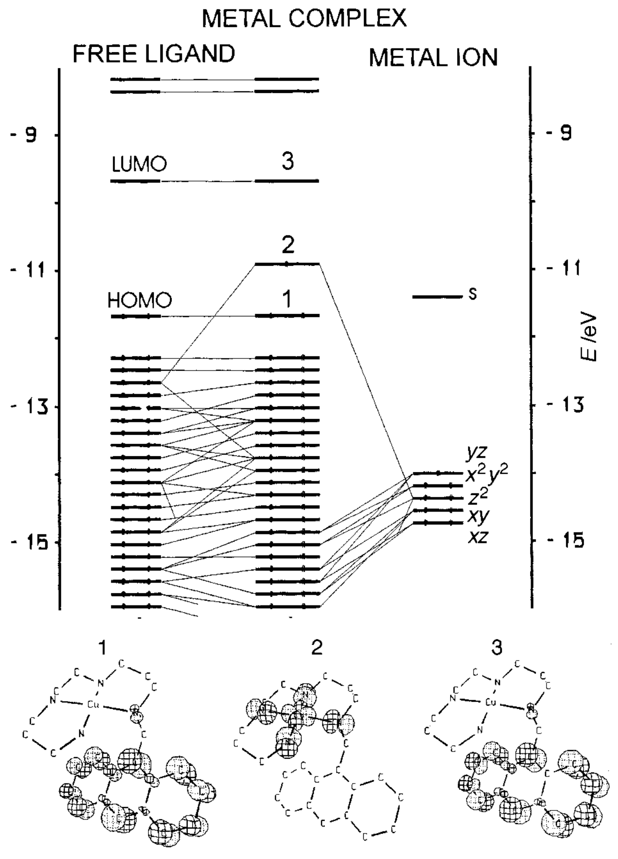

Fig. 6 Frontier molecular orbitals for the $[\mathrm{CuL}^1]^{2+}$ cation.

Zn^{2+}, similarly to H^+ (and Cd^{2+}, see below) shows a CHEF effect and that formation of hydroxo-complexes introduces a non-radiative deactivation path in the system.

The most dramatic net CHEF effect was found for Cd^{2+} where its effect is maintained at very high pH values [Fig. 5(c)]. This can be attributed to the absence of hydroxo-complexes which are present in the Zn^{2+} system.

The CHEF effect of Zn^{2+} and Cd^{2+} allows one to conclude that these metals are not as efficient as copper or nickel in deactivating the excited state. Two reasons can in principle explain this behaviour: (i) the absence of charge transfer absorption bands involving the metal, and/or (ii) the small influence of these metals (d^{10}) to assist non-radiative processes. According to the results of molecular orbital calculations, both frontier orbitals of the Zn^{2+} and Cd^{2+} complexes are located in the anthracene and no charge transfer is expected, as confirmed by the absorption spectra. Another aspect of the Zn^{2+} and Cd^{2+} behaviour concerns their capacity, along with H^+, to prevent the intramolecular electron transfer quenching process. It may be argued that any co-ordination of a substrate having positive charge and involving the lone pairs of the nitrogen into the co-ordination binding is, in principle, effective for the protection of the intramolecular electron transfer quenching. What makes Zn^{2+}, Cd^{2+} as well as H^+, efficient in promoting CHEF effects seems to be the absence of other mechanisms able to increase the rate of the non-radiative processes of the excited state. In particular, for Cd^{2+} the existence of a heavy atom effect increasing the rate of a non-radiative process seems to be precluded, on the basis of the experimentally observed increase of the emission upon co-ordination.

As mentioned in the Introduction, there is a great demand for analytical methods capable of measuring very small concentrations of pollutants in general and heavy metals in particular. As observed in Fig. 5, L^1 seems to be very attractive because not only is it water soluble, but also allows the use of the very sensitive fluorescence emission method over a wide pH region (concentrations of the order of 10^{-6} mol dm^{-3} can be easily detected). Differentiation between Cu^{2+}, Ni^{2+} and Cd^{2+}, Zn^{2+} is easy owing to the opposite effects they have on fluorescence emission. Selective detection of Cu^{2+} can be attained on the basis of the much larger thermodynamic stability of its complexes that yield CHEQ effects at much lower pH value than for Ni^{2+}. Finally, differentiation of Zn^{2+} and Cd^{2+} can be achieved at pH values >10 where emission is still observed for the Cd^{2+}–L^1 system, while the Zn^{2+}–L^1 system shows no emission due to the formation of hydroxylated species.

When comparing the behaviour of L with that of L^1 it can be verified that the latter is more appropriate as a chemosensor for Zn^{2+}, Cu^{2+} and Ni^{2+}. This is due to the fact that the association constants with these metals are much lower for L than for L^1 and thus the changes on the fluorescence emission titration curves are not so significant. However, for Cu^{2+}, the CHEQ effect leads to a higher limit of the association constant of 15 logarithm units.

Acknowledgements

We are indebted to DGICYT Project no. PB96-0796-CO2 and Portuguese Junta Nacional de Investigação Cientifica e Tecnologica (Praxis XXI/Bd/4504/94) for financial support.

References

1 J. M. Lehn, *Supramolecular Chemistry, Concepts and Perspectives*, VCH, Weinheim, 1996.
2 V. Balzani and F. Scandola, Supramolecular Photochemistry, Ellis Horwood, Chichester, 1991.
3 *Fluorescent Chemosensors for Ion and Molecule Recognition*, ed. W. Czarnik, ACS, Symposium Series 538, American Chemical Society, Washington DC, 1992; *Chemosensors for Ion and Molecule Recognition*, eds. J. P. Desvergne and A. W. Czarnik, Kluwer, Dordrecht, 1997.
4 M. E. Huston, E. U. Akkaya and A. W. Czarnik, *J. Am. Chem. Soc.*, 1989, **111**, 8735; E. U. Akkaya, M. E. Huston and A. W. Czarnik, *J. Am. Chem. Soc.*, 1990, **112**, 3590; S. A. Van Arman and A. W. Czarnik, *J. Am. Chem. Soc.*, 1990, **112**, 5376.
5 L. Fabbrizzi, M. Licchelli, P. Pallavicini, A. Perotti, A. Taglietti and D. Sacchi, *Chem. Eur. J.*, 1996, **1**, 75; L. Fabbrizzi, M. Licchelli, P. Pallavicini and A. Taglietti, *Inorg. Chem.*, 1996, **35**, 1733; L. Fabbrizzi, M. Licchelli, P. Pallavicini and L. Parodi, *Angew. Chem., Int. Ed. Engl.*, 1996, **35**, 1733.
6 R. A. P. de Silva and S. A. de Silva, *J. Chem. Soc., Chem. Commun.*, 1986, 1709; R. A. Bissell, A. P. de Silva, H. Q. N. Gunaratne, P. L. M. Lynch, G. E. M. Maguire and K. R. A. S. Sandanayake, *Chem. Soc. Rev.*, 1992, **21**, 18; R. A. Bissell, A. P. de Silva, H. Q. N. Gunaratne, P. L. M. Lynch, C. P. McCoy, G. E. M. Maguire and K. R. A. S. Sandanayake, *Top. Curr. Chem.*, 1998, **37**, 800; A. P. de Silva, H. Q. N. Gunaratne, T. Gunnlaugsson, C. P. McCoy, J. T. Rademacher and T. E. Rice, *Chem. Rev.*, 1997, **97**, 1515.
7 L. R. Sousa and J. M. Larson, *J. Am. Chem. Soc.*, 1977, **99**, 307; J. M. Larson and L. R. Sousa, *J. Am. Chem. Soc.*, 1978, **100**, 1943.
8 H. Shizuka, K. Takada and T. Morita, *J. Phys. Chem.*, 1980, **84**, 994.
9 H. Bouas-Laurent, A. Castellan, M. Daney, J.-P. Desvergne, G. Guinand, P. Marsau and M.-H. Riffaud, *J. Am. Chem. Soc.*, 1986, **108**, 315.
10 B. Valeur, J. Bourson, J. Pouget, M. Kaschke and N. P. Nernsting, *J. Phys. Chem.*, 1992, **96**, 6545.
11 M. A. Bernardo, A. J. Parola, F. Pina, E. Garcia-España, V. Marcelino, S. V. Luis and J. F. Miravet, *J. Chem. Soc., Dalton Trans.*, 1995, 993.
12 (*a*) M. A. Bernardo, J. A. Guerrero, E. García-España, S. V. Luis, J. M. Llinares, F. Pina, J. A. Ramirez and C. Soriano, *J. Chem. Soc., Perkin Trans. 2*, 1996, 2335; (*b*) M. A. Bernardo, F. Pina, E. García-España, J. Latorre, S. V. Luis, J. M. Llinares, J. A. Ramirez and C. Soriano, *Inorg. Chem.*, 1998, **37**, 3935.
13 M. I. Burguete, B. Escuder, S. V. Luis, J. F. Miravet, M. Querol and E. García-España, *Tetrahedron Lett.*, 1998, **39**, 3799.
14 M. Micheloni, A. Sabatini and A. Vacca, *Inorg. Chim. Acta*, 1977, **25**, 41.
15 E. García-España, M.-J. Ballester, F. Lloret, J.-M. Moratal, J. Faus and A. Bianchi, *J. Chem. Soc., Dalton Trans.*, 1988, 101.
16 M. Fontanelli and M. Micheloni, *Proceedings of the I Spanish–Italian Congress on Thermodynamics of Metal Complexes*, Diputación de Castellón, Castellón, Spain, 1990.

17 G. Gran, *Analyst* (*London*), 1952, **77**, 881; F. J. Rossotti and H. Rossotti, *J. Chem. Educ.*, 1965, **42**, 375.

18 A. Sabatini, A. Vacca, A. Gans and P. Gans, *Coord. Chem. Rev.*, 1992, **120**, 389.

19 C. Mealli and D. Proserpio, *J. Chem. Educ.*, 1990, **67**, 399.

20 M. S. Lehman and F. K. Larsen, *Acta Crystallogr.*, *Sect. A*, 1978, **30**, 580; D. F. Grant and E. J. Gabe, *J. Appl. Crystallogr.*, *Sect. A*, 1978, **11**, 114.

21 A. C. T. North, D. C. Philips and F. S. Mathews, *Acta Crystallogr.*, *Sect. A*, 1968, **24**, 351.

22 *Crystallographic Computing*, eds. G. M. Sheldrick, C. Kruger and R. Goddard, Clarendon Press, Oxford, 1985, p. 175.

23 G. M. Sheldrick, SHELXS-93: Program for Crystal Structure Refinement, Institute für Anorganische Chemie de Universitat, Göttingen, 1993.

24 *International Tables for X-Ray Crystallography*, Kynoch Press, Birmingham, 1974, vol. IV.

25 C. K. Johnson, ORTEP, Report ORNL-3794, Oak Ridge National Laboratory, Oak Ridge, TN, 1971.

26 A. Andrés, M. I. Burguete, E. García-España, S. V. Luis, J. F. Miravet and C. Soriano, *J. Chem. Soc.*, *Perkin Trans. 2*, 1993, 749; A. Bianchi, B. Escuder, E. García-España, S. V. Luis, V. Marcelino, J. F. Miravet and J. A. Ramírez, *J. Chem. Soc.*, *Perkin Trans. 2*, 1994, 1253.

27 E. Martell, R. M. Smith and R. J. Motekaitis, *NIST Critically Selected Stability Constants of Metal Complexes Database*, NIST Standard Reference Database, version 4, 1997.

28 J. E. Sarnesky, H. L. Surprenant, F. K. Molen and E. N. Reiley, *Anal. Chem.*, 1975, **47**, 2116; A. Bencini, A. Bianchi, E. García-España, M. Micheloni and J. A. Ramírez, *Coord. Chem. Rev.*, 1999, in press.

29 A. Andrés, C. Bazzicalupi, A. Bianchi, E. García-España, S. V. Luis, J. F. Miravet and J. A. Ramírez, *J. Chem. Soc.*, *Dalton Trans.*, 1994, 2995.

30 B. Altava, M. I. Burguete, S. V. Luis, J. F. Miravet, E. García-España, V. Marcelino and C. Soriano, *Tetrahedron*, 1997, **53**, 4751; M. I. Burguete, B. Escuder, J. C. Frías, E. García-España, S. V. Luis and J. F. Miravet, *Tetrahedron*, 1998, **63**, 1810.

31 E. García-España, J. Latorre, S. V. Luis, J. F. Miarvet, P. Pozuelo, J. A. Ramírez and C. Soriano, *Inorg. Chem.*, 1996, **35**, 4591.

Paper 8/08649D